Thermal properties and pressure-dependent elastic constants of cadmium stannate as a substrate for MEMS: An ab initio study

Nicholas Ongwen, Erick Ogam, Zine El Abiddine Fellah, Herrick Othieno, Maxwell Mageto, Henry Otunga

Thermal properties and pressure-dependent elastic constants of cadmium stannate as a substrate for MEMS: An ab initio study

*Nicholas Ongwen[1,2], Erick Ogam[3], Z. E. A. Fellah[3], Herrick Othieno[1], Maxwell Mageto[4], Henry Otunga[1]

[1]*Maseno University, P. O. Box Private Bag, Maseno, 40137, Kenya.*

Tel: +254 – 57 – 351620/22, Email: info@maseno.ac.ke

[2]*Tom Mboya University, P. O. Box 199, Homa-Bay, 40300, Kenya.*

Tel: +254 746401706, Email: principal@tmuc.ac.ke

[3]*Laboratoire de Mécanique et d'Acoustique, LMA-UMR 7031 Aix-Marseille University-CNRS-Centrale Marseille, F-13453 Marseille CEDEX 13, France.*

Tel: (+33) 4 84 52 56 00, Email: lma[at]lma.cnrs-mrs.fr

[4]*Masinde Muliro University of Science and Technology, P. O. Box 190, Kakamega, 50100, Kenya*

Tel: +254 (0) 702597360, +254 (0) 702597361, Email: info@mmust.ac.ke

Corresponding author: apache.nc.22@gmail.com, +254 715292028. P. o. Box 304-40603, Ngiya

Keywords: thermal properties; cadmium stannate; pressure-dependent elastic constants; thermal properties of cadmium stannate; substrates for MEMS; ductile MEMS substrates

Abstract

Silicon carbide (SiC) has become a suitable replacement to silicon as a substrate for manufacture of microelectromechanical systems (MEMS) that operate in harsh environmental conditions, owing to its better mechanical properties such as excellent wear resistance. However, just like silicon, SiC is also brittle, a property that limits its application as a substrate for manufacture of flexible MEMS. In this study, we explored the thermal properties as well as the pressure-dependent elastic constants of cadmium stannate (Cd_2SnO_4) for the first time within the quantum espresso code. The result showed that the elastic constants of SiC are much higher than those of Cd_2SnO_4. The properties of SiC were found to be more sensitive to the applied pressure compared those of Cd_2SnO_4, implying that it is less mechanically and thermally stable with the applied pressure compared to Cd_2SnO_4, and therefore, less appealing compared to Cd_2SnO_4 for manufacture of most MEMS.

1.0 Introduction

The world of microelectromechanical systems (MEMS) is becoming mature enough to handle the current and future demands regarding its manufacturing techniques as well as the right substrate materials for the MEMS devices. Silicon (Si) is becoming less attractive as a substrate for the manufacture of MEMS devices due to it narrower band gap, brittleness, as well as its loss of mechanical reliability in harsh environmental conditions such as at high temperatures of above 500 ^{o}C (Cimalla, Pezoldt and Ambacher, 2007) (Gerberich et al., 2012). These harsh-environment MEMS include sensors and actuators such as those in combustion processes, gas turbine control, and oil industry. The main advantages of micro components compared to the conventional macro components include their higher reliability, affordability as well as their ability to incorporate more complex functions (Varadan, 2003).

Silicon carbide (SiC) is an excellent wide band gap semiconductor with better mechanical, chemical and thermal stability. It has already been explored as a substrate material for MEMS. Moreover, it has already been incorporated into the Si micromachining technology (Cimalla, Pezoldt and Ambacher, 2007). The much higher Youngs modulus of SiC of 410-422 GPa (Messaoud et al., 2019) (Reddy, 2007) implies that it can maintain a linear relationship between the applied load and the induced deformation compared to Si, which has an effective Youngs modulus of only 130 GPa (Hopcroft, Nix and Kenny, 2010). Moreover, SiC has a large ratio of Young's modulus to density, which results to higher resonant frequencies with better quality factors for beam structures (Coakley, Splett and Janezic, 2003). This property is particularly useful for micromechanical resonators as frequency filtering in high communication transceivers. Downhole pressure sensors and diesel engine in-cylinder pressure sensor movement applications operate under high pressure regions of above 0.3 GPa.

However, one of the main shortcomings of SiC as a MEMS material is it brittleness, just like Si. It is therefore not suitable for manufacture of flexible MEMS such as sensors, actuators, micro fluidic components, and biomedical MEMS. Previous studies have shown that flexible substrates are sensitive to temperature and therefore, only low-temperature materials such as polymers are currently being utlilized for such MEMS (Tu, 2014). In this study, we explored the pressure-dependent elastic constants as well as thermal properties of cadmium stannate (Cd_2SnO_4), a wide band gap and flexible semiconductor, which is a highly attractive candidate as a substrate for the manufacture of MEMS sensors and actuators. To the best of our knowledge, there is no record on both pressure-dependent elastic constants as well as thermal properties of Cd_2SnO_4. For comparison, we also present the same properties for SiC. The specific objectives of the study were (i) to find out the effect of applied pressure on the elastic constants of Cd_2SnO_4, (ii) to determine the melting temperature of Cd_2SnO_4, and (iii) to investigate the thermal properties of Cd_2SnO_4. The rest of the paper is organized as follows: In section

two, we present the materials and methods that were employed in order to determine the elastic constants as functions of the applied pressure as well as the thermal properties of Cd_2SnO_4 and SiC. In section three, we present the main findings from the study as well as discussion of the results. The conclusions of the main findings are presented in section four.

2.0 Materials and methods

2.1 Structural optimization

The calculation of elastic constants was performed within the generalized gradient approximation (GGA) as implemented in the quantum espresso code (Giannozzi et al., 2017). The crystallographic files for both compounds were obtained from the crystallography open database (Crystallography.net). The orthorhombic Cd_2SnO_4 adopts a pbam space group (number 55), while the cubic SiC adopts an F-43m space group (number 216). The experimental lattice parameters for Cd_2SnO_4 were: a = 10.484 a.u, b = 18.693 a.u and c = 6.039 a.u, with a unit cell volume of 1,183.508 $a.u^3$ (Troemel, 1969). For the SiC cell, the experimental lattice parameter was a = 8.2401 a.u, with a unit cell volume of 559.4966 $a.u^3$ (Burdick and Owen, 1918). The 3D structures of the two unit cells are shown in figure 1.

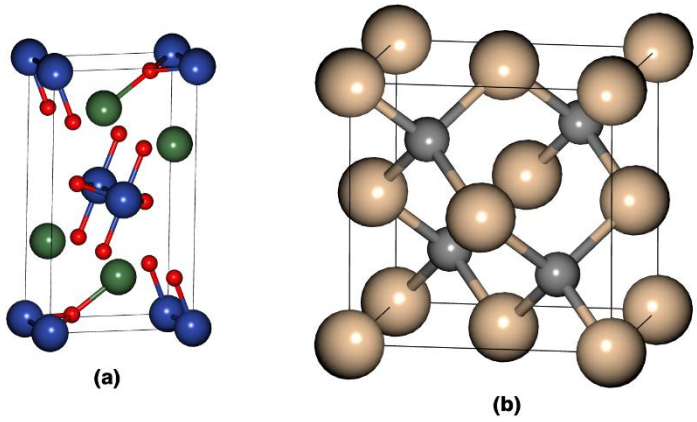

Figure 1: The crystal structures of (a) The orthorhombic cadmium stannate and (b) The cubic silicon carbide as viewed in Burai, a GUI for quantum espresso. The green spheres represent the cadmium

atoms, the blue spheres represent the tin atoms, the red spheres represent the oxygen atoms, the brown spheres represent the silicon atoms, while the grey spheres represent the carbon atoms.

The interactions between electrons and ions were described by scalar-relativistic, norm-conserving ultrasoft pseudopotentials. The GGA by Perdew-Burke-Ernzerhof functional for SOLids (PBESOL) functionals (Yoyo, Hiroyuki, Yu, Isao and Fumiyaso, 2017) were used for both cells. The Kohn-Sham wave functions were expanded on a plane-wave basis set up to a kinetic energy cut-off of 60 Ry with a total energy accuracy of 2.1 x 10^{-3} Ry for Cd_2SnO_4. For SiC, we used a kinetic energy cut-off of 80 Ry with a total energy accuracy of 1.8 x 10^{-4} Ry. The Brillouin zone integration was performed over an unshifted 5 x 3 x 9 Monkhorst-Pack mesh for Cd_2SnO_4 and 8 x 8 x 8 for SiC (Monkhorst and Pack, 1976). For optimization of atomic coordinates, variable cell relaxation was performed on the input files using the BFGS algorithm.

2.2 Calculation of elastic constants as a function of pressure

The stress-stain method by Ongwen, Ogam, and Otunga (2021) was applied in the calculation of elastic constants at the applied pressures of 0, 10, 20, 30, 40 and 50 GPa. Small strains were applied to the crystals so as to remain within the linear regime of the Hooke's law. The strains were varied from -0.006 to 0.006 in steps of 0.003 (5 data points), after which stresses were generated. The calculated stress-strain data were fitted (linear fit) in order to obtain the elastic stiffness constants (c_{ij}). Understanding of the internal strains in a material can be made possible by application of the Kleinman's equation (Kleinman, 1962). The equation is expressed as:

$$\zeta = \frac{c_{11}+8c_{12}}{7c_{11}+2c_{12}}, \qquad (1)$$

where c_{11} and c_{12} are elastic stiffness constants. The elastic stiffness constant c_{11} is related to elasticity of the length (linear resistance to compression), while c_{12} is related to the shape of the crystal.

Melting temperature (T_m) of a material is the temperature at which a solid changes into a liquid. It depends on the strength of the bonds holding the atoms of the solid together, where stronger bonds result into higher values of T_m. T_m can be determined from the relationship between the elastic stiffness constants as (Parvin and Naqib, 2019):

$$T_m = 607 + 9.31\ B \qquad (2)$$

where *B* is the bulk modulus.

2.3 Calculation of thermal properties

Thermal properties of the two compounds were determined within the quasi-harmonic approximation (Allen, 2020). The Debye temperature, also known as the characteristic temperature, is the temperature at which a pure cubic crystal's atomic heat is equal to 5.67 calories per gram of atoms per degree. It is a fundamental property of matter that governs a variety of solid properties, including specific heat, electric conductivity, thermal conductivity, X-ray spectral line widening, and elastic properties. The Debye model for the heat capacity of solids explains the specific heat capacity of solids at low temperature in terms of the quantum statistical mechanics of an ensemble of harmonic oscillators. At these temperatures, the solid can be viewed as a gas of non-interacting quasi-particles, which perfectly conforms to the Bose-Einstein statistics, which relates to the phonons. The phonon and frequency are connected by the Lyddane-Sachs-Teller relation (Kittel, 2005) (Degheidy, Elkenany, Madkour and AbuAli, 2018). For a harmonic oscillator of angular frequency ω, its internal energy in thermal equilibrium at temperature T is given by (Baroni, Giannozzi and Isaev, 2009):

$$E = \frac{h\omega}{4\pi} + \frac{h\omega}{2\pi e^{\frac{h\omega}{2\pi k_B T}} - 1} \qquad (3)$$

Upon differentiation of equation (3) with respect to temperature the sum over all the possible values of the phonon momentum in the Brillouin zone (BZ), we obtain the specific heat capacity of a solid at constant volume as:

$$c_V = \frac{1}{V}\sum_{qv}\frac{h\omega}{2\pi}(\mathbf{b},v)p'(\mathbf{b},v), \qquad (4)$$

where $\omega(\mathbf{b},v)$ is the frequency of the v-th mode (phonon) at point q in the BZ. $p'(\mathbf{b},v)$ is given by the expression: $p'(\mathbf{b},v) = \frac{\partial}{\partial T}\left[e^{\frac{h\omega}{2\pi}(\mathbf{b},v)/k_B T} - 1\right]^{-1}$, and the sum is extended to the first BZ (a uniquely defined primitive cell in the reciprocal space). If it is assumed that there are three degenerate modes at each point on the BZ, each with frequency $\omega(\mathbf{b},v) = c|\mathbf{b}|$, where c is the sound velocity, and then convert the sum in equation (4) into an integral, we end up with an expression for the specific heat capacity at constant volume in the form:

$$c_v(T) = \frac{1}{\phi}\,\frac{12\pi^4}{5}\,k_B\left(\frac{T}{\Theta_D}\right)^3, \qquad (5)$$

where ϕ is the volume of the unit cell. The symbol Θ_D is the Debye temperature, which is given by:

$$\Theta_D = \left(\frac{h}{k_B}\right)c\left(\frac{3}{4\pi\phi}\right)^3 \qquad (6)$$

The Gibbs free energy (G) of a crystal can be determined from the relation:

$$G(Z,T) = U(Z) + \frac{1}{2}\sum_{\mathbf{b}v}\frac{h(\mathbf{b},v|Z)}{2\pi} + k_B T\sum_{\mathbf{b}v}\log\left[1 - e^{\frac{h\omega(\mathbf{b},v|Z)}{2\pi k_B T}}\right], \qquad (7)$$

where Z indicates any global static constraint upon which vibrational frequencies may depend, and $U_0(Z)$ is the zero-temperature energy of the crystal as a function of Z.

3.0 Results and discussion

3.1 Structural properties

Figure 2 shows the graphs of total energy per atom against the normalized unit cell volumes for the two compounds at zero GPa pressure, which shows that SiC has much lower total energy per atom compared to Cd_2SnO_4. By fitting the volume data of the two compounds into the third order Birch-Murnaghan equation of state (Birch, 1947), the equilibrium lattice parameters for the two crystals were obtained.

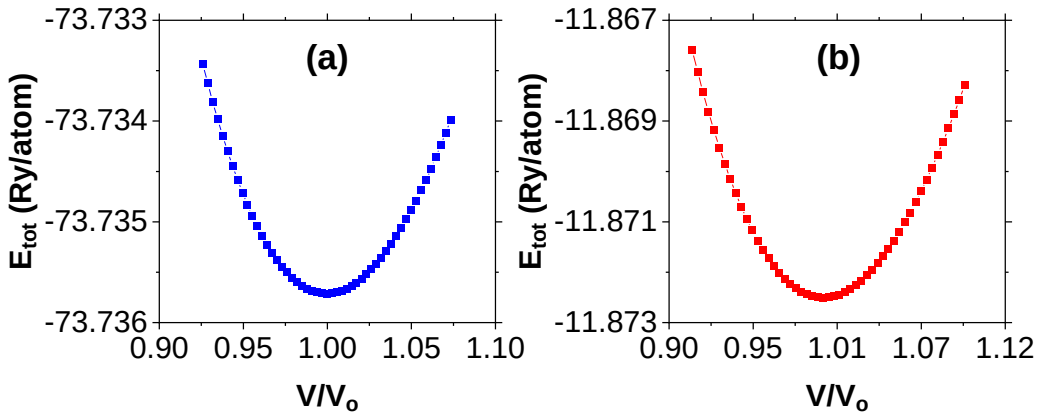

Figure 2: Total energy per atom against normalized unit cell volume at zero GPa pressure for: (a) cadmium stannate, and (b) silicon carbide.

Table 1 shows the variation of the lattice parameters extracted from figure 2, the bulk moduli, and the densities of Cd_2SnO_4 and SiC with the applied pressure. The table shows that the calculated values in this work are in excellent agreement with those of the previous studies at 0 GPa pressure. Although it is common knowledge that GGA overestimates the values of the lattice parameters compared to the experimental values and hence, underestimation of the bulk moduli, the same was not observed in the present study. This can be attributed to the improvement in the accuracy of the pseudopotentials as well as the ab initio calculations over time. The density of Cd_2SnO_4 calculated in this study is observed to be

much higher (2.37 times) than that of SiC. However, there is no record in the literature about the density of Cd_2SnO_4 at the moment for comparison. This study thus forms the basis for future reference.

Table 1: The calculated lattice parameter (a), the bulk modulus (B), the derivative of the bulk modulus with respect to pressure (B'), and the density (ρ) of the two compounds as a function of the applied pressure.

Material	p (GPa)	a (Å)	B (GPa)	B'	ρ (kg/m^3)
Cd_2SnO_4	0	5.574 (5.567[a]) (5.573[b])	149.4 (150.3[b])	4.42	7630.52
	10	5.267	191.3	4.22	
	20	5.229	496.4	15.0	
	30	5.218	731.4	15.0	
	40	5.213	968.1	15.0	
	50	5.209	1203.6	15.0	
SiC	0	4.357 (4.36[c])	221.8 (222[d])	4.03	3215.89 (3210[c])
	10	4.297	262.2	4.03	
	20	4.246	302.5	4.03	
	30	4.203	342.8	4.03	
	40	4.174	427.3	5.13	
	50	4.163	578.8	7.13	

(a) Experimental data from [Jeyadheepan and Sanjeeviraja, 2014]

(b) Computational data from [Ongwen, Ogam and Otunga, 2021]

(c) Data from [Jiang and Cheung, 2009]

(d) Data from [Clayton, 2010]

Both compounds experienced a decrease in the lattice parameters with increase in the applied pressure. Cd_2SnO_4 underwent a 6.548% shrinkage, while SiC underwent a 4.660% shrinkage when the applied pressure increased from 0 to 50 GPa. This implies that the volumes of the crystals reduce as the applied pressure increases. The shrinkage of the lattice parameters with increase in the applied pressure has also been reported (Manyali and Sifuna, 2019). The fact that Cd_2SnO_4 shrunk more than SiC for the same amount of the applied pressure implies that Cd_2SnO_4 is more compressible compared to SiC.

3.2 Pressure-dependent elastic constants

Table 2 shows the elastic stiffness constants of the two compounds as a function of the applied pressure. For orthorhombic Cd_2SnO_4, we have the nine independent elastic stiffness constants (c_{11}, c_{22}, c_{33}, c_{44}, c_{55}, c_{66}, c_{12}, c_{13} and c_{23}), while for the cubic SiC, the elastic stiffness constants reduce to three ($c_{11} = c_{22} = c_{33}$, $c_{44} = c_{55} = c_{66}$, and $c_{12} = c_{13} = c_{23}$). The elastic stiffness constants of both crystals increased with increase in the applied pressure. SiC possesses much higher elastic stiffness constants than Cd_2SnO_4. Since large values of the elastic stiffness constants imply high incompressibility, it implies that SiC is much more incompressible than Cd_2SnO_4, and thus, a greater external force is needed to deform it, which can be confirmed by the lower decrease in its lattice parameter in table 1. For Cd_2SnO_4, c_{33} is slightly larger than c_{11}, implying that there are slightly stronger bonds along the [001] direction than along the [100] direction. As the applied pressure increases, the bonds between the atoms become shorter for both crystals, a phenomenon that leads to resistance in the change in their volumes. This consequently leads to an increase in their elastic stiffness constants with increase in the applied pressure.

Table 2: The calculated elastic stiffness constants (in GPa) of cadmium stannate and silicon carbide as functions of the applied pressure

Material	p (GPa	c_{11}	c_{22}	c_{33}	c_{44}	c_{55}	c_{66}	c_{12}	c_{13}	c_{23}
Cd_2SnO_4	0	268.6	186.1	272.4	62.9	29.2	58.5	117.8	99.3	104.2
	10	322.3	206.9	312.8	67.5	32.3	70.0	171.1	141.9	148.9
	20	331.7	210.0	322.2	68.0	33.3	71.7	176.3	150.1	158.7
	30	334.7	213.0	324.0	68.1	33.6	72.3	178.3	152.5	158.8
	40	336.0	216.0	324.2	68.2	33.5	72.4	179.0	153.5	159.0
	50	336.7	217.0	324.4	68.4	33.6	72.5	179.7	154.1	159.7
SiC	0	387.5	387.5	387.5	139.3	139.3	139.3	243.9	243.9	243.9
	10	426.5	426.5	426.5	177.0	177.0	177.0	260.0	260.0	260.0
	20	461.7	461.7	461.7	212.4	212.4	212.4	271.9	271.9	271.9
	30	494.3	494.3	494.3	246.9	246.9	246.9	281.3	281.3	281.3
	40	516.7	516.7	516.7	271.3	271.3	271.3	286.9	286.9	286.9
	50	525.7	525.7	525.7	281.1	281.1	281.1	289.0	289.0	289.0

The calculated elastic constants derived from the elastic stiffness constants in table 2 are presented in table 3. The formulas for the calculation of elastic constants from the elastic stiffness constants are found elsewhere (Ongwen, Ogam and Otunga, 2021). All the four elastic constants (the bulk modulus (B), the shear modulus (G), the Young's modulus (E) and the Poisson ratio(μ)) increase as the applied pressure increases. The increase in the elastic constants with increase in the applied pressure has also

been reported by Elkenany (2021). The bulk modulus of Cd_2SnO_4 is lower than that of SiC. This shows that it is less incompressible compared to SiC. Both compounds become more incompressible with increase in the applied pressure. The bulk modulus of Cd_2SnO_4 increases by 34.91% for the increase in the applied pressure from 0 to 50 GPa, while that of SiC increase by 63.38% within the same pressure range. This indicates that SiC becomes much more incompressible with increase in the applied pressure. Higher values of the bulk modulus are in high demand for sensors and actuators that work under harsh environment. The shear modulus, which increases with increase in the applied pressure, indicates that the materials become more resistant to shape change. The shear modulus of Cd_2SnO_4 increases by 4.84%, while that of SiC increases by 10.06%, implying that SiC becomes much more resistant to shape change compared to Cd_2SnO_4.

Table 3: The calculated elastic constants of cadmium stannate as functions of the applied pressure. G is the shear modulus (in GPa), E is the Young's modulus (in GPa), μ is the Poisson ratio, n is the Pugh's ratio, and H_V is the Vickers hardness. ζ is the Kleinman parameter.

Material	P (GPa)	B	G	E	μ	N	H_V	ζ
Cd_2SnO_4	0	150.1 (150.3[a])	53.7 (53.7[a])	143.7 (143.8[a])	0.340 (0.341[a])	2.780 (2.802[a])	3.28 (3.16[a])	0.5724
	10	191.7	54.9	150.5	0.369	3.488	1.83	0.6508
	20	199.7	55.8	153.2	0.372	3.581	1.73	0.6514
	30	200.5	56.1	153.8	0.372	3.578	1.74	0.6524
	40	201.7	56.2	154.2	0.372	3.590	1.73	0.6524
	50	202.5	56.3	154.4	0.373	3.600	1.73	0.6532
SiC	0	222.0	185.9	435.9	0.172	1.194	31.56	0.7308

		(222[d])	(179[e])	(410-422[f])	(0.16[e])		(32[e])	
	10	260.0	193.6	465.1	0.201	1.344	27.82	0.7150
	20	295.5	198.8	486.8	0.224	1.486	24.82	0.6984
	30	329.4	202.2	503.3	0.244	1.628	22.26	0.6823
	40	353.1	204.1	512.9	0.256	1.731	20.64	0.6710
	50	362.7	204.6	516.3	0.261	1.771	20.05	0.6665

(e) Data from [Munro, 1997]

(f) Data from [Reddy, 2007]

The Young's modulus increases by 5.76% for Cd_2SnO_4 and by 18.44% for SiC. This implies that SiC becomes more resistant to longitudinal tension with increase in the applied pressure compared to Cd_2SnO_4. The ductility of the two compounds was tested using both the Poisson's ratio as well as the Pugh's ratio. For the Poisson's ratio, a value of 0.27 and above implies that a material is ductile, while a value of less than 0.27 shows that the material is brittle. For the Pugh's ratio, a value of more than 1.75 is an indication of ductility, while a value of less than 1.75 indicates brittleness (Pugh, 1954). From table 3, we observe that Cd_2SnO_4 is ductile at 0 GPa pressure, while SiC is brittle. Both materials become more ductile with increase in the applied pressure. SiC just reaches the boundary of ductility/ brittles (1.771) at 50 GPa pressure, while Cd_2SnO_4 becomes much more ductile as the applied pressure approaches 50 GPa.

The Poisson's ratios of the two crystals increase by 9.71 % and 51.74 % for Cd_2SnO_4 and SiC respectively, while the Pugh's ratios increase by 29.50 % and 48.32 % for Cd_2SnO_4 and SiC respectively. Although both materials become more ductile at high pressures, there is a corresponding

drop in their Vickers hardness, which implies that they become less hard, with lower wear resistance and hence, more vulnerable to scratch and abrasion, a property that is not desirable for MEMS such as micromotors and coating materials (Jiang and Cheung, 2009). The Vickers hardness decreases by 89.60% and 57.41% for Cd_2SnO_4 and SiC respectively as the applied pressure increases from 0 to 50 GPa.

The Kleinman parameter explains the resistance that a material offers against the forces that tend to stretch or bend it. As the value nears 1, it shows that the contribution of bond stretching or bond contraction to resist the applied stress becomes insignificant. It can be observed that the Kleinman parameter for SiC is closer to 1 compared to that of Cd_2SnO_4. Thus, its mechanical strength is dominated by bond stretching/ contraction. However, the Kleinman parameter values for Cd_2SnO_4 increases with increase in the applied pressure, while that for SiC decreases. This implies that the resistance that Cd_2SnO_4 offers against the forces of stretching or bending increases with increase in the applied pressure, unlike that of SiC that reduces with increase in the applied pressure. Figure 3 shows the variation of the elastic constants with the applied pressure, which shows that the elastic constants of Cd_2SnO_4 have steeper slopes than those of SiC at lower pressures, although they tend to flatten as the applied pressure increases.

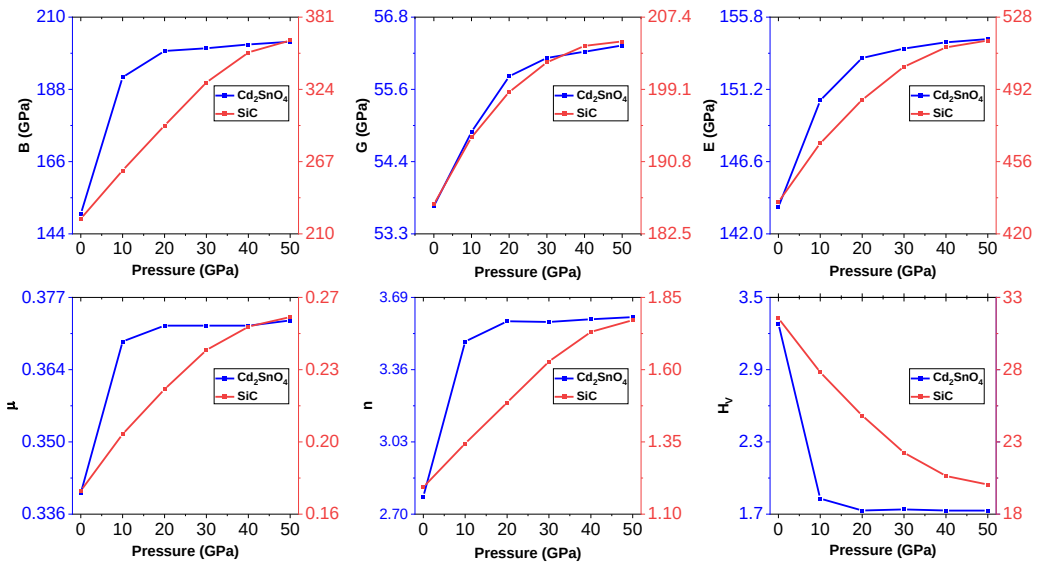

Figure 3: The computed elastic constants, the Vickers hardness (H_V) and the Pugh's ratio (n) of cadmium stannate and silicon carbide as functions of the applied pressure

3.3 Thermal properties

Table 4 shows the variation of the Debye temperatures as well as the melting temperatures of the two compounds. The higher value of the Debye temperature for SiC indicates that the optical phonons in SiC have a higher frequency than those in Cd_2SnO_4, which implies that they require greater energy to activate as compared to those of Cd_2SnO_4. This further confirms the higher stiffness of SiC compared to Cd_2SnO_4. The calculated Debye temperature of SiC obtained in this study is 3.742% lower than the value of 1194.8 K that has been reported by Peng et al. (2012). The Debye temperatures of both compounds increase with increase in the applied pressure, which implies that they become stiffer as the applied pressure increases.

Table 4. The calculated Debye temperature (Θ_D in K) and melting temperature (T_m in K)

	p (GPa)	0	10	20	30	40	50

Θ_D	Cd_2SnO_4	377.5	379.0	381.8	382.3	382.9	383.1
	SiC	1151.7	1148.9	1159.3	1165.0	1167.4	1168.0
T_m	Cd_2SnO_4	2304	2695	2769	2778	2788	2797
	SiC	2974	3328	3663	3970	4193	4287

The melting temperatures of the two compounds were calculated from their bulk moduli using equation 2, where we added the uncertainty of 300 K to the calculated values so as to obtain a good match between the experimental values that already exist in the literature and the computed values for SiC obtained in this study. As table 4 shows, the calculated melting temperature of SiC is 4.338% lower than that reported by Munro (1997) at 3103 K. We therefore calculated the melting temperature of Cd_2SnO_4 using the same formula. The higher melting temperature of SiC shows that it has greater intermolecular forces and therefore, least vapour pressure compared to Cd_2SnO_4.

The relatively higher melting temperature of Cd_2SnO_4 compared to that of silicon at 1687 K (Yang and Jiang, 2005) shows that it is also suitable for high-temperature applications. However, the values obtained in this study can be treated as an estimate, since the formula used in calculating them has a large uncertainty of 300 K. Unfortunately, there is no data in the literature for comparison with the melting temperature of Cd_2SnO_4. This study thus forms a basis for future reference. There is a consistent increase in the melting temperature with increase in the applied pressure for both compounds. This is because as the applied pressure increases, the strength of interatomic forces that exist between the atoms of the compounds increases (as already been observed in the elastic constants). This makes it more difficult for the atoms to break away from one another, leading to higher melting temperature.

Since the quasi-harmonic Debye model remains fully applicable within the temperature range of 0 to 800 K, the thermal properties in this study were calculated within the same range. Figure 4a shows the

Debye vibrational energy for Cd_2SnO_4, which increases non-linearly with temperature below 200 K. This in contrast to the Gibb's free energy (figure 4b), which decreases non-linearly within the whole temperature range. The entropy (figure 4c) tends to zero at 0 K, which implies that there is very little or no lattice disorder at 0 K temperature, which is in line with the third law of thermodynamics (the law states that the entropy of perfect crystals tends to zero at the absolute zero temperature). With increase in temperature, the system becomes disorderly and thus, the entropy increases.

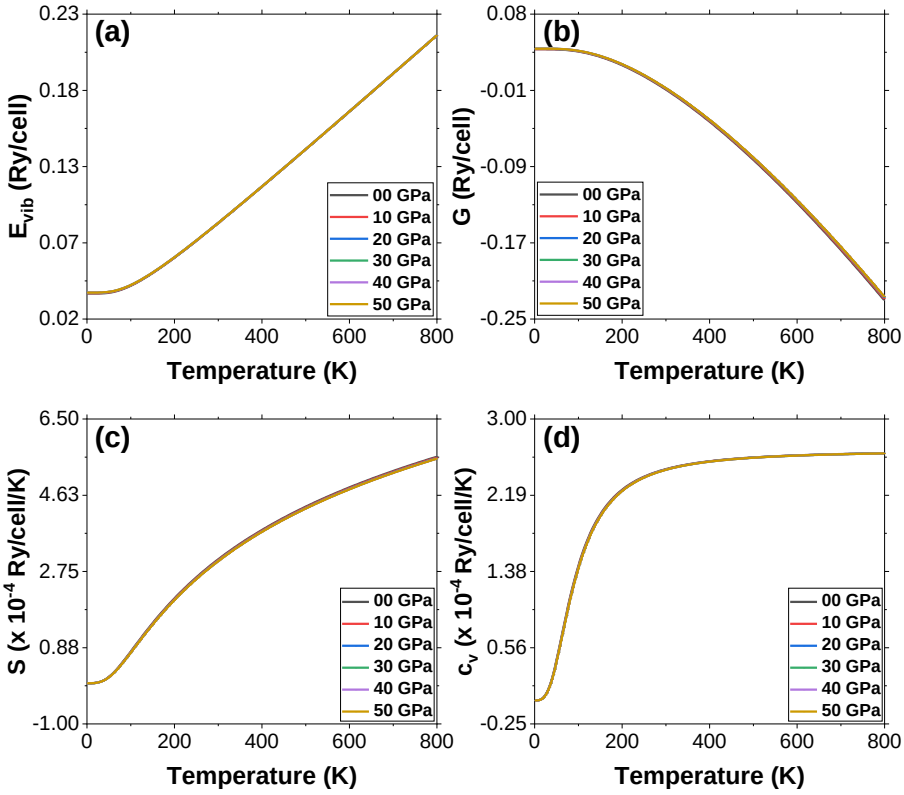

Figure 4: Thermal properties of cadmium stannate. E_{vib} is the vibrational energy, G is the Gibbs free energy, S is the entropy, and c_v is the specific heat capacity at constant volume

Specific heat capacity of a material relates to the absorption of heat. The specific heat capacity at constant volume (figure 4d) tends to zero as the absolute temperature tends to zero. This is quite in agreement with the Debye model (Kittel, 1996). The specific heat capacity of Cd_2SnO_4 exhibits a cubic

dependence of temperature as the temperature tends to zero. This implies that the phonon contribution is predominant here. The sharp increase in the specific heat capacity with temperature up to about 300 K is due to phonon thermal vibrations. As the temperature rises above 500 K, the anharmonic effect is suppressed and thus, the specific heat capacity approaches the Dulong-Petit classical limit (Dulong and Petit, 1819). At the intermediate temperature between 200 to 400 K, the atomic lattice vibrations are the main contributors to the specific heat capacity.

Figure 5 shows the variation of the thermal properties of SiC with temperature. The trend for the vibrational energy curve (figure 5a) is similar to that of Cd_2SnO_4 in figure 4a, except that the curve become linear at a higher temperature (beyond 200 K) as compared to that of Cd_2SnO_4 that becomes linear at about 100 K. Moreover, pressure seems to have a significant effect on the vibrational energy of SiC, especially at low temperature (the curves separate), a phenomenon that is not observed in Cd_2SnO_4 (figure 4a). Just as with Cd_2SnO_4, the Gibbs free energy for SiC (figure 5b) decreases non-linearly with increase in temperature. However, pressure exhibits an effect on the Gibbs free energy, as the Gibbs free energy increases with increase in the applied pressure, a phenomenon that is not observed for Cd_2SnO_4 (figure 4b).

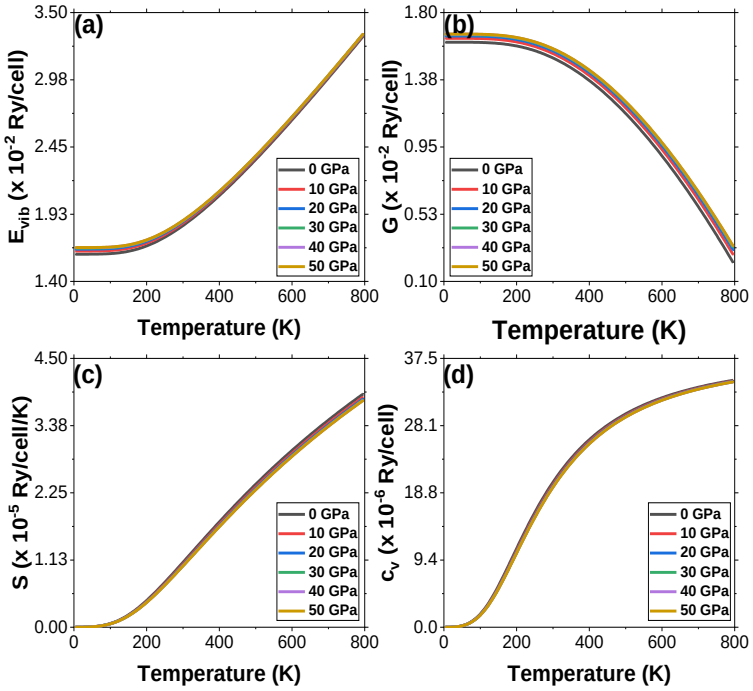

Figure 5: Thermal properties of silicon carbide. E_{vib} is the vibrational energy, G is the Gibbs free energy, S is the entropy and c_v is the specific heat capacity at constant volume

Just as for Cd_2SnO_4 (figure 4c), the entropy for SiC (figure 5c) tends to zero as temperature tends to zero. However, unlike for Cd_2SnO_4 where the pressure seems not to have an effect on the entropy, the entropy for SiC decreases with increase in the applied pressure at high temperature. The specific heat capacity of SiC also tends to zero as the temperature tends to zero (figure 5d), although the effect of pressure is not prominent in this case. Thus, both elastic and thermal properties of SiC have been found to be more sensitive to the applied pressure compared to those of Cd_2SnO_4. Table 5 shows the calculated thermal properties of Cd_2SnO_4 and SiC in this study.

Table 5: The calculated thermal properties of cadmium stannate and silicon carbide. E_{vib} and G are in Ry/cell, while S and c_v are in Ry/cell/K

Compound	E_{vib} (x 10^{-2})	G (x 10^{-2})	S (x 10^{-4})	c_v (x 10^{-4})

Cd_2SnO_4	8.557	-0.452	3.024	2.462
SiC	1.832	1.515	0.107	0.201

4.0 Conclusion

The results of this study showed that both the mechanical properties (bulk modulus, shear modulus, Young's modulus and Vickers hardness) and thermal properties (Debye temperature and melting temperature) of SiC are much higher than those of Cd_2SnO_4. It is thus ideal for the manufacture of MEMS for harsh environmental conditions. However, just like Si, SiC in this study has shown to be both mechanically and thermally unstable. It undergoes a significant change in elastic and thermal properties with change in the applied pressure. Cd_2SnO_4 on the other hand, undergoes a much lower change in its elastic as well as thermal properties as the applied pressure changes. Both materials become ductile with increase in the applied pressure. SiC just reaches the ductile/ brittle boundary of 1.75 (Pugh's ratio) at the applied pressure of 50 GPa (up from 1.34 at 0 GPa), while Cd_2SnO_4 is highly ductile even at 0 GPa pressure, with a Pugh's ratio of 2.78, and it increases to 3.60 at 50 GPa pressure. Thus, Cd_2SnO_4 can be a better substrate to SiC in the manufacture of flexible MEMS such as sensors, actuators, microfluidic components and biomedical MEMS, owing to its ductile nature. Moreover, since it is both mechanically and thermally more stable than SiC, it can form a better substrate for manufacture of downhole pressure sensors and diesel engines. However, due to its small ratio of Young's modulus to density, it is not ideal for manufacture of micromechanical resonators. The much lower Vickers hardness of Cd_2SnO_4 implies that it is not suitable for manufacture of MEMS micromotors and coating materials, which require super hard substrates.

Author contribution

Nicholas Ongwen: conceptualized the paper, performed the ab initio calculations, analyzed the results and wrote the paper. Erick Ogam: conceptualized the paper, analyzed the results and proofread the paper. Z. E. A Fellah: analyzed the results and proofread the paper. Maxwell Mageto: conceptualized and proofread the paper. Henry Otunga: proofread the paper. Andrew Oduor: proofread the paper.

Acknowledgement

The authors would like to acknowledge the center for high performance computing (CHPC), South Africa for providing the computational resources for carrying out this study.

References

1. Allen, P. B. (2020). Theory of thermal expansion: Quasi-harmonic approximation and corrections from quasi-particle renormalization. *Modern Physics Letters B, 34*(2), 2050025. Doi: https://doi.org/10.1142/S0217984920500256.
2. Baroni, S. Giannozzi, P., and Isaev, E. (2009). Thermal properties of materials from ab initio quasi-harmonic phonons. *Reviews in Mineralogy & Geochemistry, 71*, 1-19.
3. Birch, F. (1947). Finite elastic strain of cubic crystals. *Physical Review, 71*(11), 809-824.
4. Burdick, C. L., and Owen, E. A. (1918). The atomic structure of carborundum determined by X-rays. *Journal of the American Chemical Society, 40*, 1749-1759.
5. Cimalla, V. Pezoldt, J., and Ambacher, O. (2007). Group III nitride and SiC based MEMS and NEMS: Materials properties, technology and applications. *Journal of Physics D: Applied Physics, 40*(20), 6386-6434. doi: 10.1088/0022-3727/40/20/S19.
6. Clayton, J. D. (2010). *A geometrically non-linear model of ceramic crystals with defects applied to silicon carbide (SiC)*. Maryland: U.S. Army Research Laboratory.

7. Coakley, K. J. Splett, J. D., and Janezic, M. D. (2003). Estimation of Q-factors and resonant frequencies. *IEEE Transactions on Microwave Theory and Techniques, 51*(3), 862-868.
8. Crystallography.net. home page. *http://www.crystallography.net*
9. Degheidy, A. R. Elkenany, E. B. Madkour, M., and AbuAli, A. M. (2018). Temperature dependence of phonons and related crystal properties in InAs, InP and InSb zinc-blende binary compounds. *Computational Condensed Matter*. https://doi.org/10.1016/j.cocom.2018.e00308.
10. Dulong, P. L., and Petit, A. T. (1819). Reseches sur queques points importans de la theories de la chaleur. *Annales de Chimie et de Physique, 10*, 395-413.
11. Elkenany, E. B. (2021). Energy band structure, acoustic velocities, optical phonon frequencies and mechanical properties of $InP_{1-x}Sb_x$ alloys under temperature and pressure. *Infrared Physics and Technology, 115*, 103720(1-13).
12. Hopcroft, M. A. Nix, W. D., and Kenny, T. W. (2010). What is the Young's Modulus of Silicon? *Journal of Microelectromechanical Systems, 19*(2), 229-238.
13. Gerberich, W. W. Stauffer, D. D. Beaber, A. R., and Tymiak, N. I. (2012). A brittleness transition in silicon due to scale. *Journal of Materials Research, 27*(3), 552-561.
14. Giannozzi, P. Andreussi, O. Brumme, T. Bunau, O. Buongiorno, M. Calandra, M. et al. (2017). Quantum espresso: A modular and open-source software project for quantum simulations of materials. *Journal of Physics: Condensed Matter, 29*(46), 1-30.
15. Jeyadheepan, K., and Sanjeeviraja, C. (2014). Preparation and crystal structures of some $A^{IV}B_2^{II}O_4$ compounds: powder X-ray diffraction and Rietveld analysis. *Journal of Chemistry 2014*, 1-6. Doi: http://dx.doi.org/10.1155/2014/245918.

16. Jiang, L. and Cheung, R. (2009). A review of silicon carbide development in MEMS applications. *International Journal of Computational Materials Science and Surface Engineering, 2*(3/4), 225-240. DOI: 10.1504/IJCMSSE.2009.027484.
17. Kittel, C. (2005). Introduction to solid state physics. New York: John Wiley and Sons.
18. Kittel, C. (1996). *Introduction to solid state physics*. New York: John Wiley and Sons.
19. Kleinman, L. (1962). Deformation potentials in silicon. I. Uniaxial strain. *Physical Review, 126*(6), 2614-2621.
20. Manyali, G. S., and Sifuna, J. (2019). Low compressible β-BP_3N_6. *AIP Advances 9*, 125029 (1-5). Doi: https://doi.org/10.1063/1.5129268.
21. Messaoud, J. B. Michaud, J-F. Certon, D. Camarda, M. Piluso, N. Colin, L. Barcella, F., and Alquier, D. (2019). Investigation of the Young's modulus and the residual stress of 4H-SiC circular membranes on 4H-SiC substrates. *Micromachines (Basel), 10*(12), 1-12. Doi: 10.3390/mi10120801.
22. Monkhorst, H. J., and Pack, J. D. (1976). Special points for Brillouin zone integration. *Physical Review B, 13*, 5188.
23. Munro, R. G. (1997). Material properties of a sintered α-SiC. *Journal of Physical and Chemical Reference Data, 26*(5), 1195-1203. Doi: https://doi.org/10.1063/1.556000.
24. Ongwen, N. Ogam, E., and Otunga, H. (2021). Ab initio study of elastic properties of orthorhombic cadmium stannate as a substrate for the manufacture of MEMS devices. *Materials Today Communications*, 26, 101822. https://doi.org/10.1016/j.mtcomm.2020.101822.
25. Parvin, F., and Naqib, SH. (2019). Structural, elastic, electronic, thermodynamic, and optical properties of layered $BaPd_2As_2$ pnictide superconductor: A first principles investigation. *Journal of Alloys and Compounds, 780*, 452-460.

26. Pugh, S. F. (1954). XCII. Relations between the elastic moduli and the plastic properties of polycrystalline pure metals. *The London, Edinburgh, and Dublin Philosophical Journal of Science*, 45(367), 823-843. https://doi.org/10.1080/14786440808520496.
27. Reddy, J. D. (2007). *Mechanical properties of silicon carbide (SiC) thin films*. (Graduate thesis and dissertations). https://scholarcommons.usf.edu/edt/210.
28. Troemel, M. (1969). Die kristallstruktur der verbindungen vom Sr_2PbO_4-typ. *Zetschrift fuer Anorganische und Allegemeine Chemie*, *371*(5-6), 237-247.
29. Tu, H. (2007). *Flexible MEMS: A novel technology to fabricate flexible sensors and electronics*. Michigan: Wayne State University.
30. Varadan, V. K. (2003). Nanotechnology: MEMS and NEMS and their applications to smart systems and devices. *Proceedings of the SPIE*, *5062*, 20-43.
31. Yang, C. and Jiang, Q. (2005). Effect of pressure on melting temperature of silicon and germanium. *Materials Science Forum*, 475-479, 1893-1896. https://doi.org/10.4028/www.scientific.net/MSF.475-479.1893.
32. Yoyo, H. Hiroyuki, H. Yu, K. Isao, T. and Fumiyasu, O. (2017). Comparison of approximations in density functional theory calculations: Energetics and structure of binary oxides. *Physical Review B*, *96*(9), 1-24.